J Mater Sci (2017) 52:6917–6927

Influence of ethylene glycol vapor annealing on structure and property of wet-spun PVA/PEDOT:PSS blend fiber

Xinyue Wang[1,2], Gu-yu Feng[1,2], and Ming-qiao Ge[1,2,*]

[1] *Key Laboratory of Science and Technology of Eco-Textiles, Ministry of Education, Jiangnan University, Wuxi 214122, China*
[2] *College of Textile & Clothing, Jiangnan University, Wuxi 214122, China*

Received: 31 October 2016
Accepted: 3 January 2017
Published online: 15 March 2017

ABSTRACT

In this study, blend fibers composed of poly(vinyl alcohol) and poly(3,4-ethylenedioxythiophene):poly(styrene sulfonate) (PEDOT:PSS) were prepared via wet-spinning technology. Ethylene glycol (EG) vapor annealing was employed to improve the electrical conductivity and tensile properties of blend fibers. The effects of EG vapor annealing on structures and properties of blend fibers were investigated in detail by analyzing the changes in chemical constituent and structure, molecular structure, surface morphology, surface chemical composition, electrical conductivity, and tensile properties. FTIR spectroscopy indicates that EG vapor annealing does not change the chemical constituent and structure of blend fibers. Raman spectroscopy shows that vapor annealing leads to conformational changes of PEDOT chains from benzoid structure to quinoid structure. AFM and SEM images show that surface morphology of blend fibers become smoother after vapor annealing. XPS measurement shows that EG vapor annealing induces significant phase separation between PEDOT and PSS, forming an enriched PSS layer on the surface of blend fibers, thus leading to a thinner insulating PSS layer between PEDOT grains. This conformational change is beneficial to improve the electrical conductivity of blend fibers. The resultant blend fiber reached conductivity up to 20.4 S cm^{-1}. The mechanical properties of blend fibers were also improved by EG vapor annealing, with the Young's modulus and tensile strength increasing from 3.6 GPa and 112 MPa to 4.4 GPa and 132.7 MPa, respectively.

Address correspondence to E-mail: ge_mingqiao@126.com

DOI 10.1007/s10853-017-0756-8

Introduction

In recent years, there has been increased interest in research on organic materials used for electronic devices [1–4] and smart textiles [5]. Organic materials are flexible, low cost, and easy to process. These properties made them ideal for fabrication of both flexible devices and textiles in the form of either film or fiber.

Among various conducting polymers, poly(3,4-ethylenedioxythiophene):poly(styrenesulfonate) (PEDOT:PSS) has been regarded as a promising candidate as next-generation organic conductive material in both technological and industrial areas due to their optical transmission property, good thermal and environmental stability, and outstanding processability [3, 6–8]. There have been many articles reported on PEDOT:PSS casting films, such as Chen et al. [9] and Lang et al. [10]. Compared to films, PEDOT:PSS conductive fibers feature electromagnetic shielding property, tunable electrical conductivity, piezoelectricity, electrochemical sensing property, and charge storage capability [11–18]. Moreover, molecular chains in fibers could be oriented along fiber axial direction by drawing process, which made conductive fibers have relatively high conductivity.

PEDOT:PSS conductive fiber could be fabricated by wet-spinning technique with hundreds of meters in length. And it is possible that the preparation technique could be scaled up to an industrial process [19]. However, pure PEDOT:PSS conductive fibers are brittle as well as poor in mechanical property, which limit their utility of applications in many fields. In order to solve these problems, some organic polymers, such as polyurethane [20], polyaniline [21–23], and poly(vinyl alcohol) (PVA) [19], have been blended with PEDOT:PSS with an aim of improving mechanical properties. However, the addition of these organic polymers seriously reduces the electrical conductivity of resultant blend fibers due to their electrical insulation properties. Therefore, it is necessary to come up with effective methods to improve the electrical conductivity of these blend fibers. It is well known that doping of polar organic solvents such as ethylene glycol (EG), dimethylsulfoxide (DMSO), and sorbitol with PEDOT:PSS can significantly increase the conductivity up to 2 or 3 orders of magnitude [24, 25]. Moreover, the conductivity could be enhanced to different degrees by various doping methods. Currently, adding an amount of polar organic solvents into the spinning formulation is the most conventional method of solvent treatment. Seyedin et al. [20] reported that high elastomeric fiber composites with high electrical conductivity were successfully prepared by doping of DMSO into mixed spinning formulation composed of PU and PEDOT:PSS. Jalili et al. [5] reported that with a one-step EG-additive wet-spinning process, significant conductivity improvement on PEDOT:PSS fibers was achieved compared to untreated fibers. Okuzaki et al. [11] reported that significant conductivity enhancement of PEDOT:PSS fibers was achieved by dipping fibers in EG solution for 3 min. These conventional methods of solvent treatment have limitation on increasing the amount of polar solvent because fiber spinnability and softness will deteriorate with the increase amount of solvent [26]. Therefore, a novel method is put forward to enhance fiber conductivity without influencing fiber spinnability and softness.

Hence, in this paper, PVA aqueous solution was mixed with PEDOT:PSS aqueous dispersions to prepare PVA/PEDOT:PSS blend fibers via wet-spinning technique. After that, a novel EG vapor annealing treatment was carried out to improve the conductivity of the as-spun PVA/PEDOT:PSS blend fibers. The effects of EG vapor annealing on PVA/PEDOT:PSS blend fibers were investigated in detail by analyzing the changes in chemical components, morphology, conductivity, surface microscopic structure, surface composition and tensile properties. In addition, the mechanisms of the morphological, electrical, componential, and mechanical changes were investigated and discussed in detail.

Experimental

Materials

The 99.9% hydrolyzed PVA (DP = 3500) was provided by Kuraray Co. Ltd, Tokyo, Japan. PEDOT:PSS aqueous solution(Clevios^{TM} P) was purchased from HC Starck, Inc. Methyl alcohol and EG were analytically pure grades.

Preparation of spinning formulation

Mixed aqueous solution composed of PVA with a concentration of 100 mg mL^{-1} and PEDOT:PSS with a concentration of 5 mg mL^{-1} was prepared first. The

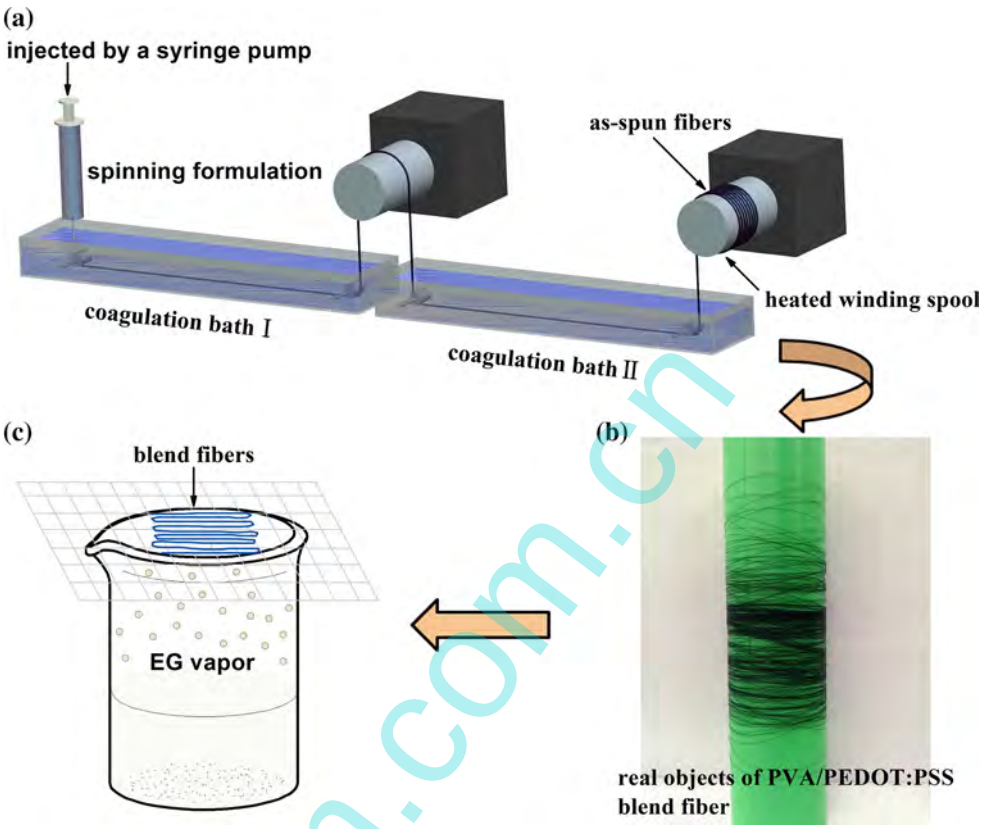

Figure 1 Preparation of PVA/PEDOT:PSS blend fiber annealed by EG vapor for different time: **a** wet-spinning apparatus, **b** real products of PVA/PEDOT:PSS blend fibers, **c** schematic graph of EG vapor annealing.

mixed aqueous solution was then homogenized at 3000 rpm (Wiggens WB3000-D) for 6 h at a constant temperature of 90 °C (IKA). After that, the homogenized mixed spinning formulation was successfully prepared.

Preparation of PVA/PEDOT:PSS blend fibers annealed for different time

The spinning formulation was injected into a 5 mL syringe and extruded into methyl alcohol coagulation bath through a needle (20 gauge) with a blunt tip. The flow rate of the spinning formulation was kept around 3.6 mL h^{-1} with the help of a syringe pump (KD Scientific). The second methyl alcohol coagulation bath functioned as washing bath for washing away the impurities inside fibers. Blend fibers that came out of coagulation baths were subsequently collected onto a heated winding spool on which temperature was set at 150 °C for drying (Fig. 1a). The linear velocity of the winding spool is 0.9 m min^{-1}. The commonly used wet-spinning apparatus in this work was shown as Fig. 1a. The real products of PVA/PEDOT:PSS blend fibers were shown as Fig. 1b. The collected blend fibers were then annealed in the atmosphere of EG vapor for different time as shown in Fig. 1c. After vapor annealing treatment, fibers were put under room temperature for drying for 24 h. In the meantime, untreated fibers were also put under the same environmental conditions as same as treated fibers. Drying samples were then used for test and characterization. For comparison, a PVA/PEDOT:PSS film with a thickness of about 100 μm was prepared by casting the homogenized mixed spinning formulation onto a glass plate and solidified at 150 °C for drying. After that, the film was put under room temperature for 24 h. As same with fiber samples, drying film samples were then used for test and characterization as well.

Characterizations

Chemical structures of blend fibers were characterized by FTIR spectrometer (Nicolet iS 10, Thermo Fisher Scientific). Electrical resistance of blend fiber was measured at room temperature using a high resistance meter (Keithley 6517B, Tektronix Company). The electrodes on the fiber were made by connecting a gold thread to the fiber surface with

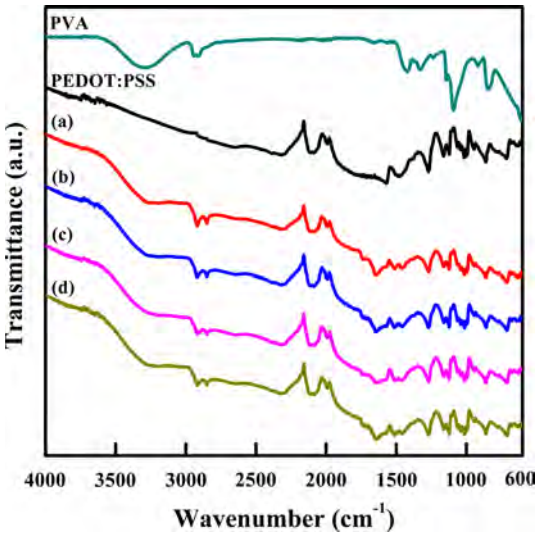

Figure 2 FTIR spectra of PVA, PEDOT:PSS, and PVA/PEDOT:PSS blend fiber annealed by EG vapor for different time: **a** 0 min, **b** 10 min, **c** 20 min, **d** 30 min.

silver epoxy. The distance between two contacts was 10 mm. For each sample, 10 different segments with same length in a roll of fibers were randomly taken and the conductivities were separately measured under the same environmental condition. The temperature-dependent conductivity measurement was performed by a two-probe method in a cryostat (PS22, Nagase) from −150 to 220 °C with a constant heating rate of 10 K min^{-1}. The Raman spectra of blend fibers were collected using a Renishaw inVia laser confocal Raman spectrometer with a 785 nm laser as an excitation source. Atomic force microscopy of blend fiber was measured using a scanning probe microscope (CSPM-3000, BenYuan Ltd) in a tapping mode over a window of 2 μm × 2 μm. The fiber was fixed on a glass slide with two pieces of adhesive tape on two ends of the fiber. Surface micro morphology of blend fibers was observed by a scanning electron microscope (SU1510, Hitachi, Japan). The mean value of fiber diameter was measured using ImageJ analysis software with 10 points taken on each fiber. The surface composition of blend fiber was measured using XPS (ESCALAB 250XI, Thermo) equipped with a monochromatic Al Kα X-ray source ($hv = 1486.6$ eV) operating at 150 W, under a high vacuum of 1×10^{-9} mbar. The tensile properties of blend fibers were measured using a tensile testing instrument (EZ-LX, Shimadzu Corporation, Japan) at a constant strain rate of 10% min^{-1}. Samples were fixed on paper cards (20 mm length window) with an adhesive tape. The Young's modulus, yield stress, tensile strength, and elongation at break were measured, and the mean and standard deviations were calculated from at least 10 tests.

Results and discussion

Effect of EG vapor annealing on the chemical structures

In order to investigate the effect of EG vapor annealing on chemical structures of PVA/PEDOT:PSS blend fiber, the Fourier transform infrared (FTIR) spectroscopy was first carried out by an FTIR spectrometer. Figure 2 shows the FTIR spectra of PVA, PEDOT:PSS, and PVA/PEDOT:PSS blend fibers annealed for different time, respectively. In the spectra of PVA, the peaks at 2947, 1330, and 849 cm^{-1} are attributed to C–H symmetrical stretching vibration, C–H in-plane bending vibration, and C–C stretching vibration of carbon chains, respectively [27, 28]. The peaks at 1420 and 1094 cm^{-1} correspond to CH–OH bending vibration and C–O stretching vibration, respectively. The absorption band around 3328 cm^{-1} is attributed to the stretching frequency of –OH group [29]. As for the spectra of PEDOT:PSS, the band at around 2100 cm^{-1} between 2300 and 1900 cm^{-1} appears in the spectrum is due to the vibration of CO_2 molecules [30]. Peaks at 1510 and 1277 cm^{-1} are assigned to the C=C and C–C stretching vibration of the thiophene ring [29]. The peaks at 1164, 1123, and 1025 cm^{-1} (two ν_{s-o} bands and one $\nu_{s\text{-phenyl}}$ band) verify the existence of sulfonic acid group [29]. Peaks at 1066 and 1040 cm^{-1} correspond to the stretching of C–O–C bonds [30]. And peaks at 952, 858, and 710 cm^{-1} are related to the stretching vibration C–S bond in the thiophene ring [29, 31]. In the spectra of pristine PVA/PEDOT:PSS blend fiber(Fig. 2a), the successful formation of blend fiber is confirmed by the presence of characteristic peaks of both PVA and PEDOT:PSS. In addition, compared to the spectra of pristine blend fiber, there are no additional functional groups in the spectra of EG vapor-annealed blend fibers (Fig. 2b–d), indicating that vapor annealing treatment does not change the chemical constituents of PVA/PEDOT:PSS blend fiber.

Effect of EG vapor annealing on the molecular structure

To explore the molecular structural changes induced by EG vapor annealing, Raman spectra of blend fibers annealed for different time were collected and studied. Figure 3 shows the Raman spectra of blend fibers annealed by EG vapor for different time. In the spectra of pristine PVA/PEDOT:PSS blend fiber(Fig. 3a), the characteristic peak at 1432 cm^{-1} was assigned to the stretching vibration of C_α=C_β on the five-member thiophene ring of PEDOT [32–34], which shifted to red and became weak after EG vapor annealing(Fig. 3b–d), indicating the conversion of resonant structure of PEDOT chain from benzoid structure into quinoid structure [35]. These conformational changes were consistent with Ouyang et al. [35]. The benzoid structure was regarded as coiled conformation, while the quinoid structure was known as linear or expanded-coil conformation [35]. According to the related theoretical model of Flory Macromolecular Solution Theory [36, 37], compared to benzoid structure, quinoid structure was more favorable for intra- and inter-chain charge transport in PEDOT, thus lowering the carrier migration energy and improving charge transport rate, which may in turn led to significant enhancement in conductivity of PVA/PEDOT:PSS blend fiber.

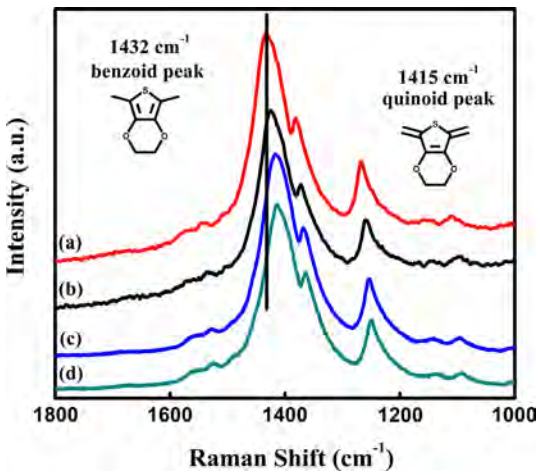

Figure 3 Raman spectra of PVA/PEDOT:PSS blend fiber annealed by EG vapor with different time: **a** 0 min, **b** 10 min, **c** 20 min, **d** 30 min.

Effect of EG vapor annealing on the surface morphology

EG vapor annealing influenced not only structures of blend fiber, but also the surface morphology of blend

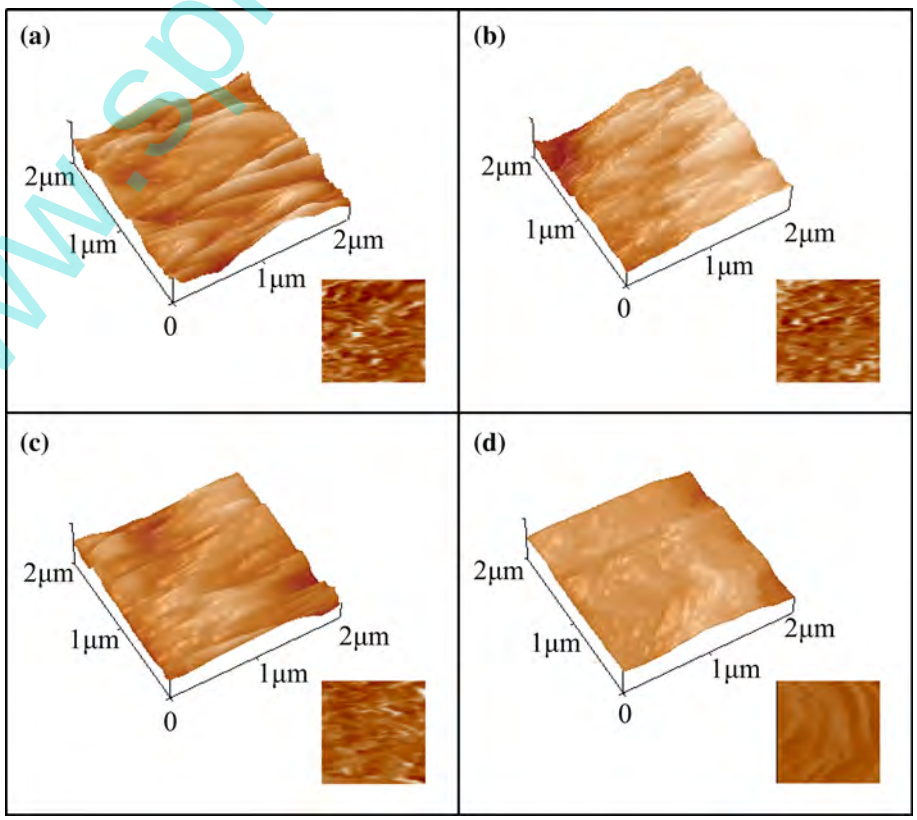

Figure 4 AFM height images of PVA/PEDOT:PSS blend fibers annealed by EG vapor for different time: **a** 0 min, **b** 10 min, **c** 20 min, **d** 30 min. The *insets* of **a**–**d** are the corresponding phase images.

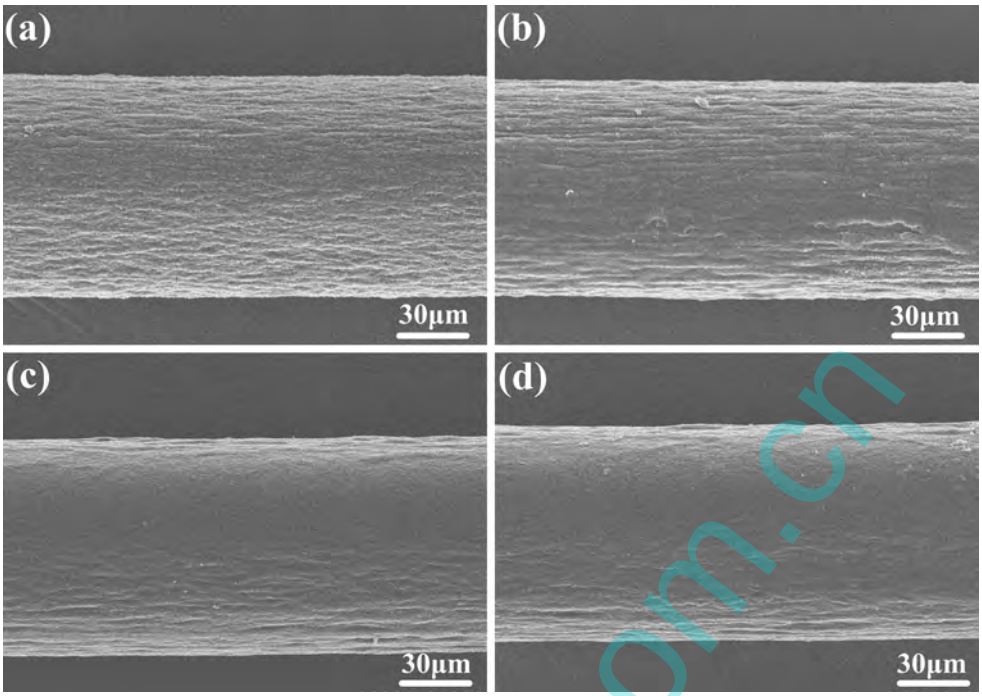

Figure 5 SEM images of PVA/PEDOT:PSS blend fibers annealed by EG vapor for different time: **a** 0 min, **b** 10 min, **c** 20 min, **d** 30 min.

fiber. Atomic force microscopy (AFM) and scanning electron microscope were employed to determine the effect of EG vapor annealing on the surface morphology of blend fiber. Figure 4a–d shows the height images of PVA/PEDOT:PSS blend fiber annealed by EG vapor for different time; the phase images are presented in the insets of Fig. 4a–d. As the annealing time increased from 0 min (pristine) to 30 min, the root-mean-square roughness of blend fiber gradually decreased from 35.8 to 18.6 nm, indicating that the surface of blend fiber became smoother after EG vapor annealing. It can be observed from phase images that as annealing time increased, the clearly revealed PEDOT grains and PSS segments in pristine blend fiber gradually became obscured, indicating that phase separation might occurred between conductive PEDOT grains and amorphous PSS segments in vapor-annealed blend fiber. The presence of PEDOT:PSS was generally regarded as conductive PEDOT grains surrounded by amorphously insulating PSS segments [36, 37]. In the pristine blend fiber, the thick and insulating PSS segments hindered the charge transport between adjacent conductive PEDOT grains [12]. After EG vapor annealing, amorphous PSS segments partially moved to the surface of blend fiber, resulting in a highly enriched component of PSS on the surface of blend fiber, as well as thinner PSS layer and better interconnection between conductive PEDOT chains [12], which may significantly improve the conductivity of PVA/PEDOT blend fiber. With respect to the AFM images, Fig. 5a–d shows the SEM images of blend fibers annealed by EG vapor for different time. Fiber diameters under different annealing time are shown in Table 1. There is no obvious change in fiber diameters. But it can be clearly observed from Fig. 5 that the surface of blend fiber became smoother as annealing time increased. The surface morphological changes observed in SEM images were consistent with the changes shown in AFM images. That is to say, amorphous PSS segments partly removed to the surface of blend fiber after EG vapor annealing, which helped to smooth the surface of blend fibers.

Table 1 Fiber diameters at different annealing time

Annealing time (min)	Fiber diameter (μm)
0	94.3 ± 0.7
10	93.9 ± 0.9
20	94.1 ± 1.2
30	93.4 ± 0.6

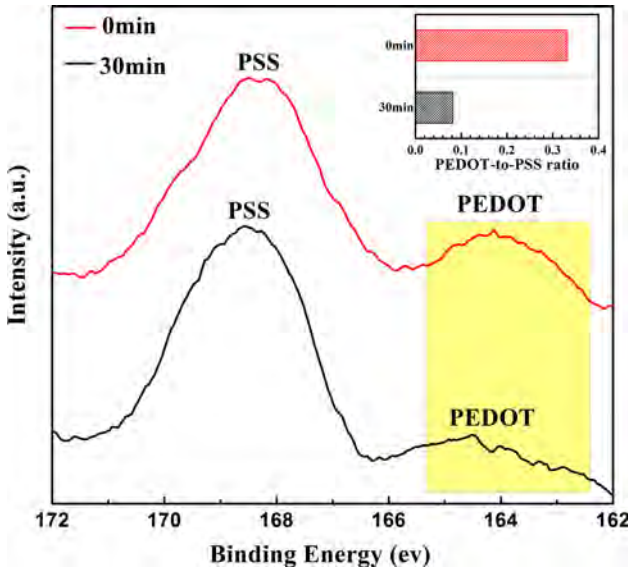

Figure 6 XPS (S_{2P}) spectra of PVA/PEDOT:PSS blend fibers annealed by EG vapor for different time. The insets are PEDOT-to-PSS ratios.

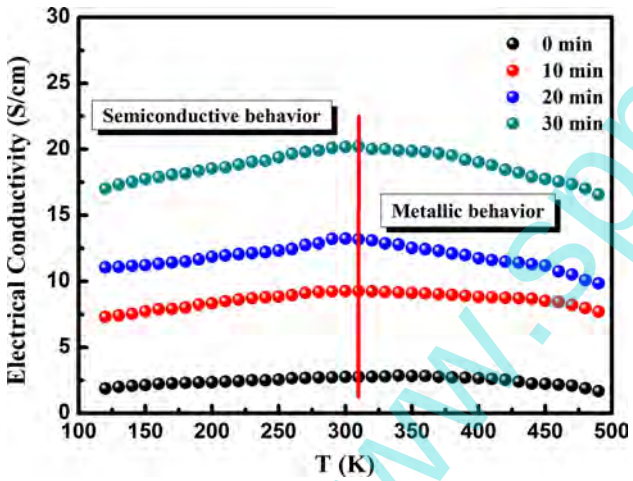

Figure 7 Temperature-dependant electrical conductivity of PVA/PEDOT:PSS blend fibers annealed by EG vapor for different time.

Effect of EG vapor annealing on the surface composition

In order to confirm the morphological changes indicated in AFM measurements, X-ray photoelectron spectroscopy (XPS) was used to explore the surface compositional changes of PVA/PEDOT:PSS blend fibers before and after EG vapor annealing. Figure 6 shows the S 2*p* spectra of PVA/PEDOT:PSS blend fibers before (0 min) and after EG vapor annealing(30 min). The S 2*p* spectra of PEDOT and the S

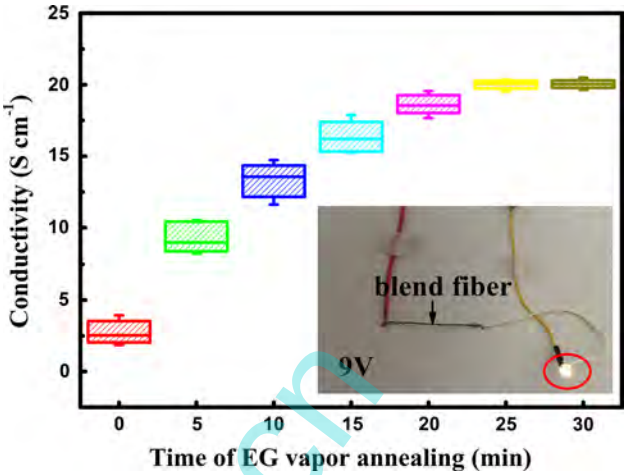

Figure 8 Conductivity of PVA/PEDOT:PSS blend fibers annealed by EG vapor for different time. The *inset* is the demonstration of an LED bubble lightened by PVA/PEDOT:PSS blend fiber that annealed by EG vapor for 30 min.

Table 2 Evaluation of conductivity stability after a period of environmental exposition

Time (h)	Conductivity (S cm^{-1})
0.5	20.0 ± 0.3
1	20.0 ± 0.1
2	19.3 ± 0.4
4	19.1 ± 0.6
8	19.8 ± 0.3
24	19.6 ± 0.1
48	19.5 ± 0.5
96	20.1 ± 0.2

2*p* spectra of PSS have different binding energies due to the sulfur atom in PEDOT existing in the thiophene ring, while the sulfur atom in PSS existing within the sulfonate fragments [38–41]. In Fig. 6, the two well-signaled peaks at around 164 and 168 eV originate from PEDOT and PSS, respectively [42]. The PEDOT-to-PSS ratio on the surface of blend fiber was calculated by area ratio of the peaks associated with PEDOT and PSS [37]. The ratios are shown in the insets of Fig. 6. It can be observed from Fig. 6 that the peak corresponding to the PEDOT moiety decreased significantly after EG vapor annealing for 30 min, and the related PEDOT-to-PSS ratio decreased sharply from 0.33 to 0.08, indicating that significant phase separation occurred between PEDOT and PSS, leading to amorphous PSS segments enrich on the surface

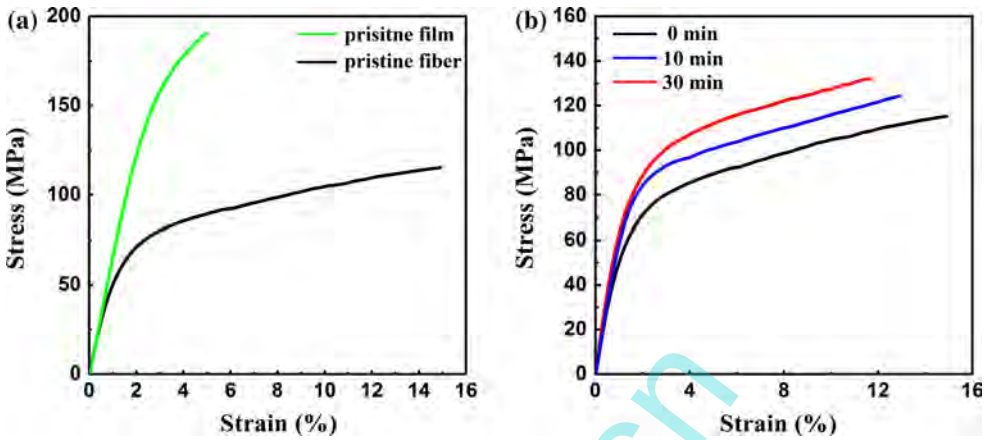

Figure 9 Representative stress–strain curves of: **a** unannealed PVA/PEDOT:PSS blend fiber with respect to unannealed PVA/PEDOT:PSS blend film, **b** PVA/PEDOT:PSS blend fiber annealed by EG vapor for different time.

of annealed blend fiber. These surface compositional changes could well confirm the morphological changes demonstrated in AFM measurements. Furthermore, phase separation between PEDOT and PSS led to insulating and amorphous PSS segments enrich on the surface of annealed blend fiber, resulting in better connection network between PEDOT due to less and thinner PSS layer acting as barrier between conductive PEDOT grains [12, 36], which might significantly improve the conductivity of PVA/PEDOT:PSS blend fiber.

Effect of EG vapor annealing on the electrical conductivity

It is well known that better chemical structure, molecular structure, morphology, or composition distribution may be more favorable for charge transport in blend fiber [36]. Therefore, in order to investigate the effects of these structural and morphological changes on electrical properties of blend fibers, the electrical properties of PVA/PEDOT:PSS blend fibers annealed for different time were measured. Figure 7 shows the temperature-dependent conductivity of blend fibers annealed for different time. It can be seen from Fig. 7 that electrical conductivity of fibers rises at low temperature range (semiconducting characteristics), while declines at high temperature range (metallic characteristics) [12]. The transition temperature is at around 310 K. It is well known that semiconductor–metal transition behavior widely exists in conductive polymers [15]. The semiconducting behavior could be regarded as carrier hopping or tunneling between PEDOT:PSS grains, while the metallic behavior indicated intrachain transport [12]. Figure 8 shows the electrical conductivity of blend fibers annealed for different time. As shown in Fig. 8, pristine blend fiber had a low conductivity around 2.5 S cm^{-1}, and the conductivity gradually improved as the vapor annealing time increased. Above an annealing time of 20 min, the conductivity remained constant above 19.2 S cm^{-1}. The conductivity was then basically remained unchanged after 25 min. A peak conductivity of 20.4 S cm^{-1} was obtained under the annealing time of 30 min. Furthermore, fiber with the peak conductivity had an amazing ability to lighten an LED bubble as shown in the inset of Fig. 8. The improvement in conductivity was well consistent with the structural and morphological changes mentioned above. On the one hand, EG vapor annealing resulted in conformational changes of PEDOT chain from benzoid structure to quinoid structure, which lowered the charge migration energy in blend fiber and in turn led to a remarkable increase in fiber conductivity [35]. On the other hand, EG vapor annealing induced significant phase separation between PEDOT and PSS, leading to a part of amorphous and insulating PSS segments enrich on the surface of blend fiber, which formed a better connection between conductive PEDOT grains due to a thinner insulating PSS layer between PEDOT grains [36]. However, over an annealing time of 30 min, the fiber conductivity showed a slight decline owing to a dewetting phenomenon [43, 44], indicating that an overlong annealing time might result in an unstable conductivity. The evaluation of conductivity stability of blend fiber under room temperature within a period of time is shown in Table 2. Fiber that annealed by EG vapor for 30 min could obtain a stably high conductivity of 20 S cm^{-1}, and this value was nearly nine times higher than that of pristine

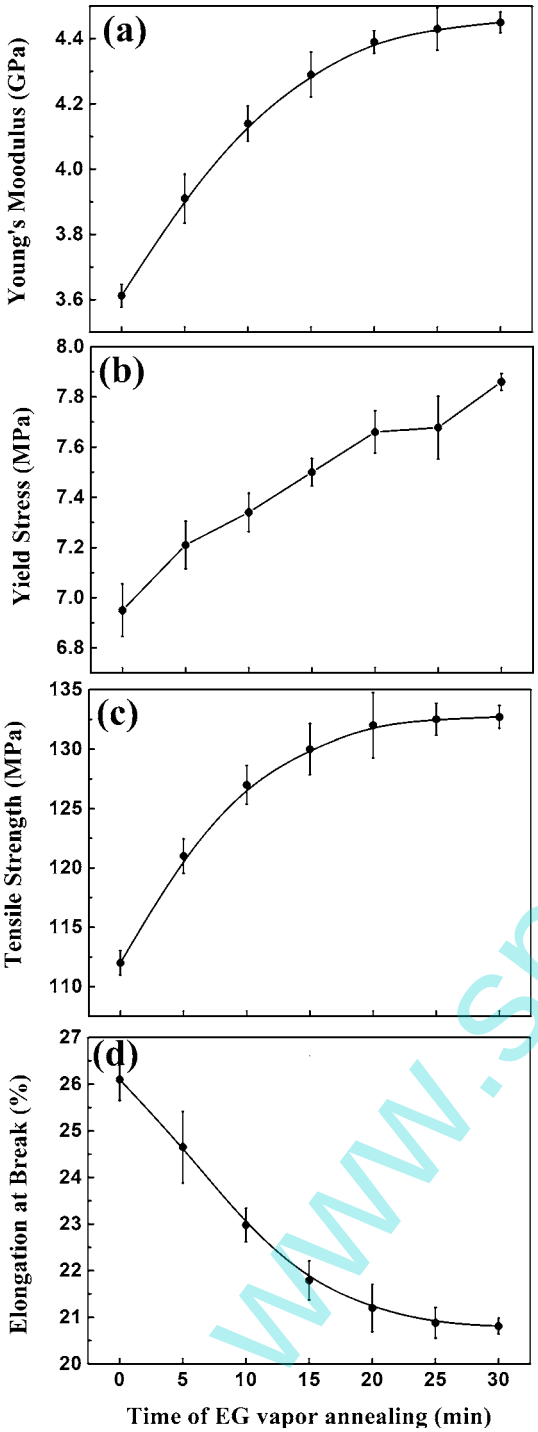

Figure 10 Tensile properties of PVA/PEDOT:PSS blend fibers annealed by EG vapor for different time: **a** Young's modulus, **b** yield stress, **c** tensile strength, **d** elongation at break.

blend fiber. Therefore, it was obvious that EG vapor annealing was an effective method to improve the conductivity of PVA/PEDOT:PSS blend fiber.

Effect of EG vapor annealing on the tensile properties

In fact, EG vapor annealing not only improved the conductivity of PVA/PEDOT:PSS blend fiber, but also enhanced the tensile properties of blend fiber. For comparison, stress–strain curves of untreated casting film with respect to untreated blend fiber are represented in Fig. 9a. It can be observed from Fig. 9a that Young's modulus (7.4 GPa) and tensile strength (190.0 MPa) of cast film were both higher than those of blend fiber. Cast film has a relatively more even structure than blend fiber due to the possible structural defects formed during the fast dehydration process within fiber [45]. Representative stress–strain curves of blend fibers annealed for 0, 10, and 30 min are shown in Fig. 9b, respectively. In order to investigate the effects of EG vapor annealing on tensile properties of blend fibers, the Young's modulus, yield stress, tensile strength, and the elongation at break of blend fibers annealed for different time were measured as shown in Fig. 10. It can be observed from Fig. 10 that tensile properties of blend fibers were dramatically improved by EG vapor annealing, with Young's modulus and tensile strength increased from 3.6 GPa and 112.0 MPa to 4.4 GPa and 132.7 MPa, respectively. This result can be explained by the conformational changes resulted from vapor annealing. EG vapor annealing made PEDOT chain converted from benzoid structure to quinoid structure, corresponding to C_α=C_β on each thiophene ring turning into C_α–C_β [46], while C_α–C_β connecting two adjacent thiophene rings turning into C_α=C_β [46]. These conformational changes weakened the internal rotation interaction of single bond, thus enhancing the molecular chain rigidity [42, 47]. Therefore, as annealing time increased, the Young's modulus of blend fiber increased, while the elongation at break of blend fiber decreased. It is understandable that the interaction among PEDOT chains with linear structure is stronger than that among PEDOT chains with coiled structure [35]. The quinoid structural PEDOT chain could intertwine with PVA chains more tightly due to its linear or expanded-coil structure, which would decrease the number of structural defects at which deformation or fractures usually took place due to stress concentration [11], and thus improved the tensile strength of blend fiber.

Conclusions

In conclusion, EG vapor annealing induced significant phase separation between PEDOT and PSS, forming an enriched PSS layer on the surface of blend fiber, leading to thinner insulating PSS layer and better connection between conductive PEDOT grains, which helped to improve the conductivity of PVA/PEDOT:PSS blend fiber. EG vapor annealing also led to conformational changes of PEDOT chain from benzoid structure to quinoid structure. The resultant PVA/PEDOT:PSS blend fiber showed an enhanced conductivity up to 20.4 S cm^{-1}. As vapor annealing time increased, the Young's modulus and tensile strength of blend fiber increased from 3.6 GPa and 112 MPa to 4.4 GPa and 132.7 MPa, respectively, while the elongation at break of blend fiber decreased.

Acknowledgements

This work was supported by the National Natural Science Funds (No. 51503082), and the National Key Research and Development Program of China (No. 2016YFB0302900).

References

[1] Na S-I, Kim S-S, Jo J et al (2008) Efficient and flexible ITO-free organic solar cells using highly conductive polymer anodes. Adv Mater 20:4061–4067

[2] Kirchmeyer S, Reuter K (2005) Scientific importance, properties and growing applications of poly(3,4-ethylenedioxythiophene). J Mater Chem 15:2077–2088

[3] Groenendaal L, Jonas F, Freitag D et al (2000) Poly(3,4-ethylenedioxythiophene) and its derivatives: past, present, and future. Adv Mater 12:481–494

[4] Spinks GM, Mottaghitalab V, Bahrami-Samani M et al (2006) Carbon-nanotube-reinforced polyaniline fibers for high-strength artificial muscles. Adv Mater 18:637–640

[5] Jalili R, Razal JM, Innis PC et al (2011) One-step wet-spinning process of poly(3,4-ethylenedioxythiophene): poly(styrenesulfonate) fibers and the origin of higher electrical conductivity. Adv Funct Mater 21:3363–3370

[6] Chan HSO, Ng SC (1998) Synthesis, characterization and applications of thiophene-based functional polymers. Prog Polym Sci 23:1167–1231

[7] Crispin X, Marciniak S, Osikowicz W et al (2003) Conductivity, morphology, interfacial chemistry, and stability of poly(3,4-ethylene dioxythiophene)–poly(styrene sulfonate): a photoelectron spectroscopy study. Polym Sci B Polym Phys 41:2561–2583

[8] Nardes AM, Kemerink M, de Kok MM et al (2008) Conductivity, work function, and environmental stability of PEDOT: PSS thin films treated with sorbitol. Org Electron 9:727–734

[9] Chen CH, Torrents A, Kulinsky L et al (2011) Mechanical characterizations of cast poly(3,4-ethylenedioxythiophene): poly(styrenesulfonate)/polyvinyl alcohol thin films. Synth Met 161:2259–2267

[10] Lang U, Naujoks N, Dual J (2009) Mechanical characterization of PEDOT: PSS thin films. Synth Met 159:473–479

[11] Okuzaki H, Harashina Y, Yan H (2009) Highly conductive PEDOT/PSS microfibers fabricated by wet-spinning and dip-treatment in ethylene glycol. Eur Polym J 45:256–261

[12] Zhou J, Li EQ, Li RP et al (2015) Semi-metallic, strong and stretchable wet-spun conjugated polymer microfibers. J Mater Chem C 3:2528–2538

[13] Cherenack K, Zysset C, Kinkeldei T et al (2010) Woven electronic fibers with sensing and display functions for smart textiles. Adv Mater 22:5178–5182

[14] Abouraddy AF, Bayindir M, Benoit G et al (2007) Towards multimaterial multifunctional fibres that see, hear, sense and communicate. Nat Mater 6:336–347

[15] Behabtu N, Young CC, Tsentalovich DE et al (2013) Strong, light, multifunctional fibers of carbon nanotubes with ultra-high conductivity. Science 339:182–186

[16] Egusa S, Wang Z, Chocat N et al (2010) Multimaterial piezoelectric fibres. Nat Mater 9:643–648

[17] Kou L, Huang T, Zheng B et al (2014) Nat Commun 5:1–10

[18] Yang ZB, Deng J, Chen XL et al (2013) A highly stretchable, fiber-shaped supercapacitor. Angew Chem Int Ed Engl 52:13453–13457

[19] Miura H, Fukuyama Y, Sunda T et al (2014) Foldable textile electronic devices using all-organic conductive fibers. Adv Eng Mater 16:550–555

[20] Seyedin MZ, Razal JM, Innis PC et al (2014) Strain-responsive polyurethane/PEDOT: PSS elastomeric composite fibers with high electrical conductivity. Adv Funct Mater 24:2957–2966

[21] Andreatta A, Caod Y, Chiang JC et al (1988) Electrically-conductive fibers of polyaniline spun from solutions in concentrated sulfuric acid. Synth Met 26:383–389

[22] Pomfret SJ, Adams PN, Comfort NP et al (2000) Electrical and mechanical properties of polyaniline fibres produced by a one-step wet spinning process. Polymer 41:2265–2269

[23] Mottaghitalab V, Xi B, Spinks GM et al (2006) Polyaniline fibres containing single walled carbon nanotubes: enhanced performance artificial muscles. Synth Met 156:796–803

[24] Yamad T, Hayamizu Y, Yamamoto Y et al (2011) A stretchable carbon nanotube strain sensor for human-motion detection. Nat Nanotechnol 6:296–301

[25] Paradiso R, Loriga G, Taccini N (2005) A wearable health care system based on knitted integrated sensors. Inf Technol Biomed IEEE Trans 9:337–344

[26] Do H, Reinhard M, Vogeler H et al (2009) Polymeric anodes from poly(3,4-ethylenedioxythiophene): poly(styrenesulfonate) for 3.5% efficient organic solar cells. Thin Solid Films 517:5900–5902

[27] Zhou J, Lubineau G (2013) Improving electrical conductivity in polycarbonate nanocomposites using highly conductive PEDOT/PSS coated MWCNTs. ACS Appl Mater Interfaces 5:6189–6200

[28] Xia Y, Sun K, Ouyang J (2012) Solution-processed metallic conducting polymer films as transparent electrode of optoelectronic devices. Adv Mater 24:2436–2440

[29] Xu Y, Wang Y, Liang J et al (2009) A hybrid material of graphene and poly(3,4-ethyldioxythiophene) with high conductivity, flexibility, and transparency. Nano Res 2:343–348

[30] Khan S, Narula AK (2016) Bio-hybrid blended transparent and conductive films PEDOT: PSS: chitosan exhibiting electro-active and antibacterial properties. Eur Polym J 81:161–172

[31] Zhang H, Xu J, Wen Y et al (2015) Conducting poly(3,4-ethylenedioxythiophene): poly(styrene-sulfonate) film electrode with superior long-term electrode stability in water and synergistically enhanced electrocatalytic ability for application in electrochemical sensors. Synth Met 204:39–47

[32] Garreau S, Louran G, Buisson JP et al (1999) In situ spectroelectrochemical Raman studies of poly(3,4-ethylenedioxythiophene) (PEDT). Macromolecules 32:6807–6812

[33] Łapkowski M, Proń A (2000) Electrochemical oxidation of poly(3,4-ethylenedioxythiophene)—"in situ" conductivity and spectroscopic investigations. Synth Met 110:79–83

[34] Garreau S, Duvail JL, Louarn G (2002) Spectroelectrochemical studies of poly(3,4-ethylenedioxythiophene) in aqueous medium. Synth Met 125:325–329

[35] Ouyang J, Xu Q, Chu CW et al (2004) On the mechanism of conductivity enhancement in poly(3,4-ethylenedioxythiophene): poly(styrene sulfonate) film through solvent treatment. Polymer 45:8443–8450

[36] Yeo JS, Yun JM, Kim DY et al (2012) Significant vertical phase separation in solvent-vapor-annealed poly(3,4-ethylenedioxythiophene): poly(styrene sulfonate) composite films leading to better conductivity and work function for high-performance indium tin oxide-free optoelectronics. ACS Appl Mat Interfaces 4:2551–2560

[37] Flory PJ, McIntyre AD (1995) Mechanism of crystallization in polymers. J Polym Sci 18:592–594

[38] Crispin X, Jakobsson FLE, Crispin A et al (2006) The origin of the high conductivity of poly(3,4-ethylenedioxythiophene)–poly(styrenesulfonate)(PEDOT–PSS) plastic electrodes. Chem Mater 18:4354–4360

[39] Zotti G, Zecchin S, Schiavon G et al (2003) Electrochemical and XPS studies toward the role of monomeric and polymeric sulfonate counterions in the synthesis, composition, and properties of poly(3,4-ethylenedioxythiophene). Macromolecules 36:3337–3344

[40] Schaarschmidt A, Farah AA, Aby A et al (2009) Influence of nonadiabatic annealing on the morphology and molecular structure of PEDOT–PSS films. J Phys Chem B 113:9352–9355

[41] Kim GH, Shao L, Zhang K et al (2013) Engineered doping of organic semiconductors for enhanced thermoelectric efficiency. Nat Mater 12:719–723

[42] Yan H, Okuzaki H (2009) Effect of solvent on PEDOT/PSS nanometer-scaled thin films: XPS and STEM/AFM studies. Synth Met 159:2225–2228

[43] Dickey KC, Anthony JE, Loo Y-L (2006) Improving organic thin-film transistor performance through solvent-vapor annealing of solution-processable triethylsilylethynyl anthradithiophene. Adv Mater 18:1721–1726

[44] Lee WH, Kim DH, Cho JH et al (2007) Change of molecular ordering in soluble acenes via solvent annealing and its effect on field-effect mobility. Appl Phys Lett 91:092105

[45] Okuzaki H, Ishihara M (2003) Spinning and characterization of conducting microfibers. Macromol Rapid Commun 24:261–264

[46] Ouyang J (2013) "Secondary doping" methods to significantly enhance the conductivity of PEDOT: PSS for its application as transparent electrode of optoelectronic devices. Displays 34:423–436

[47] Wang XJ, Perzon E, Delgado JL et al (2004) Infrared photocurrent spectral response from plastic solar cell with low-band-gap polyfluorene and fullerene derivative. Appl Phys Lett 85:5081–5083